error curve to its axis at $\Phi = 0$; $r_0\Delta\theta_0$ is the distance from the axis to the curve at $\Phi = \pi/2$; $\Delta\rho$ is the distance from the line $\Delta d = 0$ to the axis. These quantities are positive and negative, respectively, when the arrow points up and down. It may happen that no correction is indicated or possible, as occurs when the plotted points scatter about the line $\Delta d = 0$, or when errors in the data cause such a disposition of the plotted points that they will not accommodate a sine curve of the required periodicity.

Although it is hardly ever necessary, the correction procedure can be repeated by treating the corrected parameters as approximate and finding a second correction. Much time can be saved in doing this if the second error curve is deduced from the first by taking the $\Delta d$'s for the second curve as the vertical distance from the first error curve to the plotted points. This distance is positive or negative, respectively, when the plotted point in question lies above or below the first error curve. The values of $\Phi$ obtained for the first error curve may be used without alteration for the second error curve.

The magnitude of the scatter of the points about the last error curve drawn is indicative of the limits of experimental precision. From this scatter one can deduce tolerances to be put on corrected values $r_0'$, $\theta_0'$ and $\rho'$.

ACKNOWLEDGMENT

The work described in this paper was conducted under contract AF 19(122)-3 sponsored by the Air Force Cambridge Research Center. The authors wish to acknowledge helpful discussions with Dr. L. B. Felsen and Mr. H. Kurss and to thank Miss M. Eschwei for her work in the construction of Nichrome films.

# A Rotary Joint for Two Microwave Transmission Channels of the Same Frequency Band

H. P. RAABE†

*Summary*—**This paper describes a rotary joint for two microwave transmission channels of the same frequency band. It consists of two pairs of rectangular waveguide terminals, a circular waveguide which transmits both channels, and coupling elements between the rectangular waveguide terminals and the circular waveguide which convert the rectangular $H_{10}$ mode into the circular $H_{01}$ and $E_{01}$ modes. If pure $H_{01}$ and $E_{01}$ modes can be excited, perfect separation of the channels as well as constant amplitudes and phases can be obtained when the joint rotates. While the conversion into the circular $E_{01}$ mode is performed by a conventional method, a new method had to be developed for the conversion of the rectangular $H_{10}$ into the circular $H_{01}$ mode.**

## INTRODUCTION

ROTARY JOINTS for microwave transmission channels have wide application in the field of radar as a link between the stationary transmitter-receiver apparatus and the rotating antenna. Since transmitted and received power is generally guided through the same channel, only single rotary joints are required. However, complex radar systems may require double transmission and receiving channels. For such systems double rotary joints must be devised.

In this report a new type of double rotary joint (DRJ) is described which represents the class of multiple mode rotary joints. The basic idea is this: If the diameter of a circular waveguide is large enough to allow transmission of more than one circularly symmetrical mode, and if it is possible to excite any of these modes individually, there will be no crosstalk between the channels when simultaneously transmitted.

† Wright Air Dev. Center, Wright-Patterson AFB, Ohio.

## PART I: DESIGN PRINCIPLE OF THE DOUBLE ROTARY JOINT

### *Choice of Circular Modes*

That circularly symmetrical mode which requires the smallest diameter of a cylindrical waveguide is the $E_{01}$ mode. Therefore, it is the preferable mode for single rotary joints. If the diameter of the cylinder is increased the next circularly symmetrical mode which can be transmitted will be the $H_{01}$ mode. The $E_{01}$ and the $H_{01}$ modes are the most advantageous for the design of a DRJ.

Since the $E$ modes will produce a longitudinal current a contact problem exists for the circular waveguide in the plane of rotation. As space around the waveguide is available, a choke joint can easily be provided.

### *The Undesired Circular Modes*

The next and most essential problem is the design of coupling elements between standard rectangular waveguides and the circular waveguide. Coupling elements usually radiate a large number of modes. However, only

modes for which the size of the waveguide cross section is sufficiently large will be transmitted. The table in Fig. 1 shows the minimum diameter of a circular waveguide for various modes, normalized with respect to the free space wavelength. For a single rotary joint in which the $E_{01}$ mode would be used, the diameter could be chosen between 0.766 and 0.972 wavelengths, so that only one undesired mode would be transmitted if the coupling elements are not properly designed. For the DRJ using the $H_{01}$ mode in the additional channel the diameter must be chosen between 1.220 and 1.338 wavelengths as a minimum so that the circular waveguide would be able to transmit four undesired modes if the coupling elements are not properly designed.

| No. | Min. Diam / Wave L'gth | MODE | Electric Field Pattern |
|---|---|---|---|
| 1 | 0.586 | $H_{11}$ | |
| 2 | 0.766 | $E_{01}$ | |
| 3 | 0.972 | $H_{21}$ | |
| 4 | 1.220 | $E_{11}$ | |
| 5 | 1.220 | $H_{01}$ | |
| 6 | 1.338 | $H_{31}$ | |
| 7 | 1.634 | $E_{21}$ | |
| 8 | 1.693 | $H_{41}$ | |

Fig. 1—Table of the eight lowest circular modes including two circularly symmetrical modes.

*Excitation of the Circular $E_{01}$ Mode*

As far as the excitation of the $E_{01}$ mode is concerned a coupling method was chosen for the design of the DRJ as described in this report, which consists of a coaxial radiating rod in the center of the cylinder, protruding through a hole in the bottom. This method was selected because this coaxial rod can produce only radial and longitudinal (i.e. parallel to the axis of the cylinder) electrical field components. In other words, it can produce only the transverse (circular) magnetic field component and, therefore, cannot excite any of the undesired modes listed in the table of Fig. 1. A model can also easily be constructed with accuracy, and an adjustable matching device can easily be provided. Nevertheless, most of the coupling methods now used for single rotary joints can be adapted for the DRJ if they are more desirable from the standpoint of high-power handling capacity, bandwidth, or production.

*New Methods to Excite the Circular $H_{01}$ Mode*

As far as the excitation of the $H_{01}$ mode is concerned, the design of a suitable coupling method established a new problem. Since the end walls are already occupied by the coupling device for the $E_{01}$ mode, a method was designed which resulted in the excitation of the transverse currents on the inner surface of the cylindrical wall. As Fig. 2 illustrates, this current is fed in through slots from a rectangular waveguide which surrounds the cylinder. The table in Fig. 1 indicates that the minimum number of slots is three, because if the diameter of the cylinder is between 1.220 and 1.338 wavelengths a single slot would excite the modes $H_{11}$, $H_{21}$, and $E_{11}$, besides the desired mode $H_{01}$, and two slots would excite the undesired mode $H_{21}$. If it is difficult to design the DRJ with a diameter within the narrow margin mentioned above, it becomes necessary to include the $H_{31}$ mode in this consideration which would be excited by a set of three slots. In order to exclude this mode also, it would be necessary to provide four slots.

These three or four slots have to be perfectly balanced, which means that the currents entering by the slots have to be equal in amplitude and phase. Therefore, the surrounding rectangular waveguide feeding these slots has to be designed so that the distance between two adjacent slots along the rectangular guide is equal to a whole number of guide wavelengths. The surrounding waveguide is terminated by a short circuit at a half-wavelength behind the fourth slot so that maximum current density will exist around the slots.

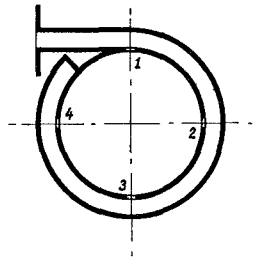


Fig. 2—Scheme of a transition for rectangular $H_{10}$ mode to circular $H_{01}$ mode. The four coupling windows are in electrical balance only for a single frequency, for which the wavelength is determined by the distance of windows.

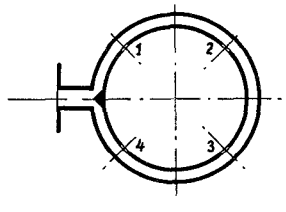


Fig. 3—Scheme of a transition for rectangular $H_{10}$ mode to circular $H_{01}$ mode. The window pairs, *1* with *4*, and *2* with *3*, are in electrical balance independent of frequency, while balance between the pairs exists only for a particular frequency for which the wavelength is determined by the distance of the windows *1* and *2* or *4* and *3* respectively.

This coupling method, of course, will limit the useful bandwidth of the DRJ, because a deviation of the frequency will unbalance the amplitude and phase of the four slots and consequently set up undesired modes. Therefore, the design of Fig. 3 will give better results. The energy will be divided into two paths at the *T*-

junction. No reflection will occur at this place if the surrounding waveguide is half as wide as the feeding waveguide, measured in the $E$-plane, and if a triangular prism of proper dimension is provided. The two waves traveling around in opposite directions will establish a node of the electrical field at the equidistant point to the $T$-junction, so that this point acts like a short circuit. Consequently slots 1 and 4 as well as slots 2 and 3 will always be balanced for any frequency, while the possible unbalance between 1 and 2 or 3 and 4, respectively, is greatly reduced compared with the possible unbalance in the system of Fig. 2. The coupling method is preferable also from the viewpoint of the construction of a model.

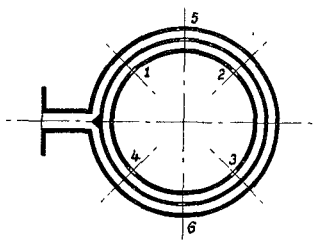


Fig. 4—Scheme of a transition for rectangular $H_{10}$ mode to circular $H_{01}$ mode. The four coupling windows *1* to *4* are in electrical balance independent of frequency, because they are at identical electrical distance from the balanced coupling windows *5* and *6*.

A further improvement along the same line of balancing the excitation of the slots is shown in Fig. 4. Two rectangular waveguides surround the circular waveguide, so that the primary, or inner, guide will serve the same purpose as the surrounding waveguide in Fig. 3. The secondary, or outer, waveguide is arranged on top of the other one. Both waveguides are coupled by slots 5 and 6 through their common walls. These slots are located at opposite points halfway between two of the four slots, 1, 2, 3, and 4 going into the circular waveguide. The secondary waveguide is again fed by a waveguide $T$-junction located halfway between the two slots 5 and 6. Since these two slots are perfectly balanced, the four sides $1 \cdots 4$ will also be perfectly balanced.

The following example shows that the effect of the two surrounding waveguide rings can be obtained in a single ring. As Fig. 5 illustrates, this ring is a square waveguide and consequently is able to support the modes $H_{01}$ and $H_{10}$. The rectangular waveguide feeder guiding the $H_{10}$ mode forms an $H$-plane $T$-junction with the ring. The resonance slot parallel to the $H$-plane at the end of the rectangular feeder, where it is tapered out to join the ring, does not restrict the transmission of this mode. From the $T$-junction two waves will be transmitted in both directions around the waveguide ring, but these $H_{10}$ waves will not excite the four slots 1, 2, 3, and 4 in the inner cylindrical wall. At the equidistant point with respect to the $T$-junction a resonance window is arranged perpendicular to the $H$-plane of this mode so that the waves will be reflected as if there were a short circuit. Thus a standing wave will be established in the ring. The dimensions of the waveguide ring are such that the electrical length of the ring is equal to four guide wavelengths. Therefore, current maxima will be found in the diametrically and symmetrically located points 5 and 6. In these places the $H_{10}$ mode can be considered as the superposition of two diagonally polarized modes. By means of slots arranged in one corner as the figure shows, the two diagonal wave components will be affected differently. Since the slots will

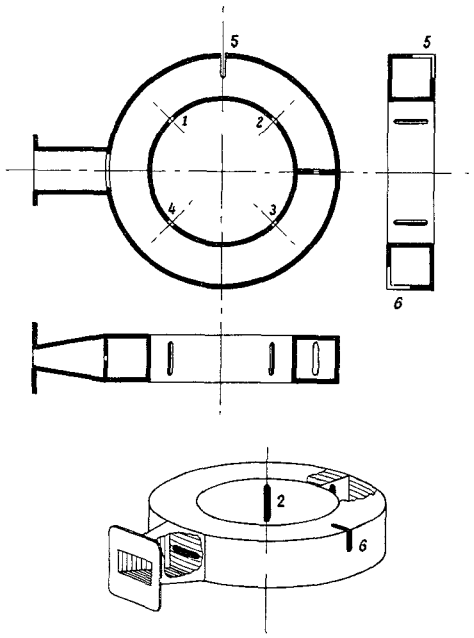


Fig. 5—Scheme of a transition for rectangular $H_{10}$ mode to circular $H_{01}$ mode. The four coupling windows *1* to *4* are in electrical balance independent of frequency because they are at identical electrical distances from the balanced points *5* and *6*, where the square mode $H_{10}$ is generated by means of resonance slots in the waveguide corner. These corners are excited by the square $H_{01}$ mode which is established at the $T$-junction of a tapered rectangular feeding guide and the ring.

stop the current flow of the diagonal mode pointing into the slotted corner, this mode will be reflected as if there were an open end. However, the other diagonal mode will not be affected. Since the diagonal modes can again be considered as the superposition of the square $H_{10}$ and $H_{01}$ modes, the slots, in effect, generate the mode $H_{01}$ and transmit it in both directions around the waveguide ring. This mode will excite the four slots $1 \cdots 4$ in a perfectly balanced manner. The window across the rectangular feeder will serve as a perfect shield for this mode, while the window at the opposite point will have no effect. It may be noted that the slots in position 5 and 6 have to be cut in adjacent corners to obtain the proper phasing. For a practical design it would be necessary to shield the radiation from slots 5 and 6 by shorted quarter-wavelength waveguide stubs. The models which have been constructed and tested utilized the coupling method illustrated in Fig. 3. Fig. 6 (opposite) shows schematically the design of the entire DRJ.

## Part II: Theory of Transmission through the Double Rotary Joint

### *Transmission through the $E_{01}$ Channel*

As pointed out above the transmission of energy through the $E_{01}$ Channel of the DRJ can be performed by a technique already established for single rotary joints. However, because of the larger diameter of the circular waveguide special care has to be taken in order to avoid excitation of any of the higher modes. The proposed design in Fig. 6 promises success, because theoretically none of the undesired modes can be excited. By tuning the rod length and the coaxial stub in series with the rod, perfect matching at the transition into the circular waveguide can be achieved at the operating frequency. The bandwidth is limited by the coupling device.

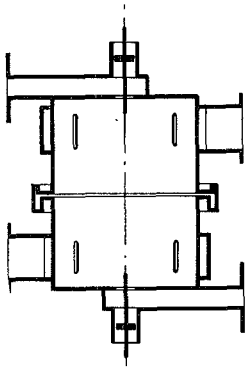

Fig. 6—Scheme of a double rotary joint.

### *Transmission through the $H_{01}$ Channel*

For the transmission of energy through the $H_{01}$ channel perfect matching at the transition into the circular waveguide is not easily achieved. However, any mismatch at one end of the DRJ can be cancelled by the mismatch at the other end if the mismatches, specifically the slots, are separated electrically by a whole number of half-wavelengths, because the waveguide section between the mismatches would then act like a 1:1 transformer. Top and bottom walls of the circular waveguide must be located at a distance of a quarter-guide wavelength from the center of the slots. This matching condition depends, of course, on frequency, and if maximum bandwidth is required a mathematical analysis of the wave transmission must be carried out.

The problem of matching the slots to the rectangular waveguide ring has been mentioned above. The match of the straight rectangular feeding waveguide to the waveguide ring can be performed over a wide band by established methods.

### *Definition of the Characteristic Impedance of the Rectangular Waveguide*

In order to analyze the transmission through the DRJ mathematically using the $H_{01}$ mode, it is useful to set up an equivalent network. Analogous to the rectangular waveguide entering and leaving the rotary joint, we have a two-wire transmission line of characteristic impedance $Z_r$, which can be arbitrarily chosen. Since the power $N$ in the transmission line must be the same as that of the waveguide system, current and voltage in the transmission line is determined by $Z_r$ and $N$. The transverse electric and magnetic field components which contribute exclusively to the transmitted power may be considered analogous to voltage and current in the transmission line. Since the transverse magnetic field in the waveguide established the longitudinal wall current, which is restricted to the wider wall, this current or current density is analogous to the transmission line current. It is simply for convenience that we make the maximum current density analogous to the line current, and calculate the characteristic impedance accordingly.

### *The Equivalent Circuit of the $H_{01}$ Channel of the Double Rotary Joint*

Fig. 7 illustrates the equivalent circuit of the $H_{01}$ channel of the DRJ. It was derived as follows. The waveguide ring is four wavelengths long. Assuming the four slots go all the way across the wider wall, that they are covered with a resistive diaphragm, and that the electric displacement current is negligibly small, the equivalent circuit would show a series resistance in the four respective positions which, in effect, would result in four times the individual resistance at the $T$-junction. In order to cancel the actual capacitive current across the slots a resonance window is used which realizes the purely resistive load. This means that resonance circuits consisting of parallel reactances to the slot resistances must be inserted in the equivalent circuit.

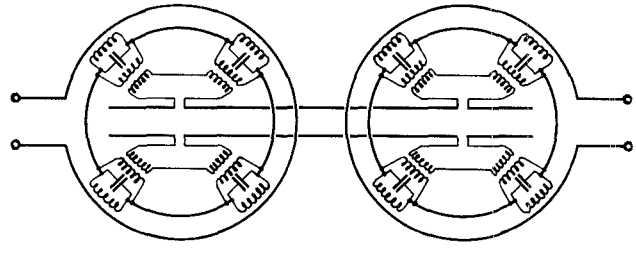

Fig. 7—Equivalent circuit for the $H_{01}$ channel of the double rotary joint.

In the next phase these slot resistances must be replaced by circuit elements of the circular waveguide. This waveguide again is represented by a two-wire transmission line. Here, the power is determined by the circular electric and the radial magnetic field. However, the circular wall current density which is excited by the four slots is equal to the longitudinal magnetic field strength next to the surface. Therefore, the circular wall-current density, preferably its peak value, must serve as analog to the transmission line current. Since the longitudinal magnetic field and, consequently, this wall current, will be zero at the top and bottom wall of

the cylinder, the termination of the equivalent transmission line is that of an open end.

With respect to the $H_{01}$ circular mode, the four slots are connected in series and act like a single one. In order to show this clearly, the current paths on the inner and outer surfaces are presented as separate conductors coupled by ideal transformers, so that the current in both coils is always the same. This circuit is somewhat unrealistic inasmuch as the current cannot differ in any of the slots, whatever the conditions may be. In the actual rotary joint a current difference is possible which will result in the excitation of undesired modes. To complete the equivalent circuit for those modes, additional transmission lines would have to be added to the slots with specific coupling circuits. Since the analysis would become extremely complicated, the equivalent circuit was simplified so that only one pair of slots was involved. If these slots are placed halfway between the rear and front pair of slots, they might have about the same effect on the frequency response as the original four slots. Because of symmetry, the lower half of the circuit can be omitted, so that the simple equivalent circuit of Fig. 8 remains.

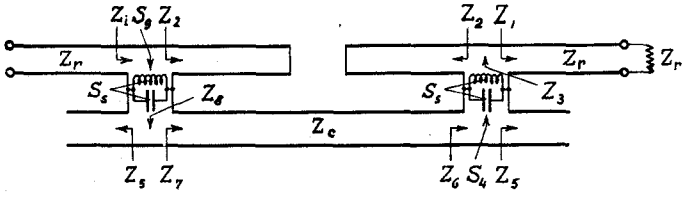


Fig. 8—Simplified equivalent circuit for the $H_{01}$ channel of the double rotary joint.

*The Characteristic Impedance of the Circular Waveguide*

In order to find the characteristic impedance of the transmission line representing the circular waveguide, we first assume, as with the rectangular guide, that the power $N$ is transmitted and completely absorbed by resistive diaphragms in the slots. Under this condition the current density in the wall can be calculated. It is a sinusoidal wave traveling parallel to the cylinder. This means that the currents entering by the slots will not feed the circular waveguide in a point, as suggested by the equivalent network. They actually excite the cylinder with partly leading and partly lagging components. This results in the excited cylinder wall-current being smaller than in the case of point excitation. Therefore, the characteristic impedance of the circular waveguide will depend not only on the wall-current density ratio between the rectangular and cylindrical waveguide, but also on the reduction factor due to the distributed excitation.

The analysis of the impedance ratio of the equivalent transmission lines has been carried out in Appendix I. The numerical value for an experimental model indicates that there is a considerable mismatch inasmuch as the characteristic impedance of the circular waveguide is 3.05 times that of the rectangular guide. Therefore, resonance oscillations are not sufficiently damped to allow broadband operation.

*The Theoretical VSWR vs Frequency Curve*

In Appendix II the VSWR has been calculated to be in the neighborhood of the operating frequency. Because of the linear shape of the experimental curve the analysis could be reduced to finding the slope of the operating frequency. Losses were also neglected. Without these simplifications the analysis would have become extremely involved. The result can be broken down into four elements referring to different parts of the DRJ. The contribution obtained from the middle section of the circular waveguide is the greatest element if the impedance ratio is large. The second positive contribution comes from the shorted rectangular waveguide stub. It is independent of the impedance ratio. A very small constant negative effect can be attributed to the resonance window, while the fourth element, which is also negative, refers to the quarter-wavelengths stubs of the circular guide and is very small for large impedance ratios. It is interesting to note that the slope may become zero for a small impedance ratio, but additional investigation is required to determine whether this condition can be realized.

## Part III: Design and Test of an Experimental Model

*Design Characteristics*

The first experimental model was based on the simple scheme of Fig. 3 where the waveguide ring is half as high as the straight rectangular waveguide feeder whose inside dimensions are 0.900 inch × 0.400 inch. However, the bandwidth was found to be too narrow due to a high theoretical mismatch of 20 between the circular waveguide and the waveguide ring. The theory indicated that with the increase of the height of the waveguide ring to twice the reference value this mismatch

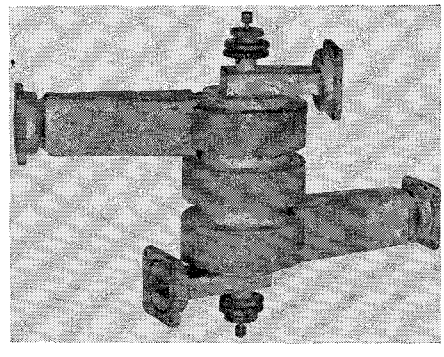

Fig. 9—Outside view of the double rotary joint.

decreases and the bandwidth increases by a factor of approximately four. Therefore, a second model was designed, which is illustrated in Fig. 9. The inside dimension of the waveguide ring was chosen the same as that

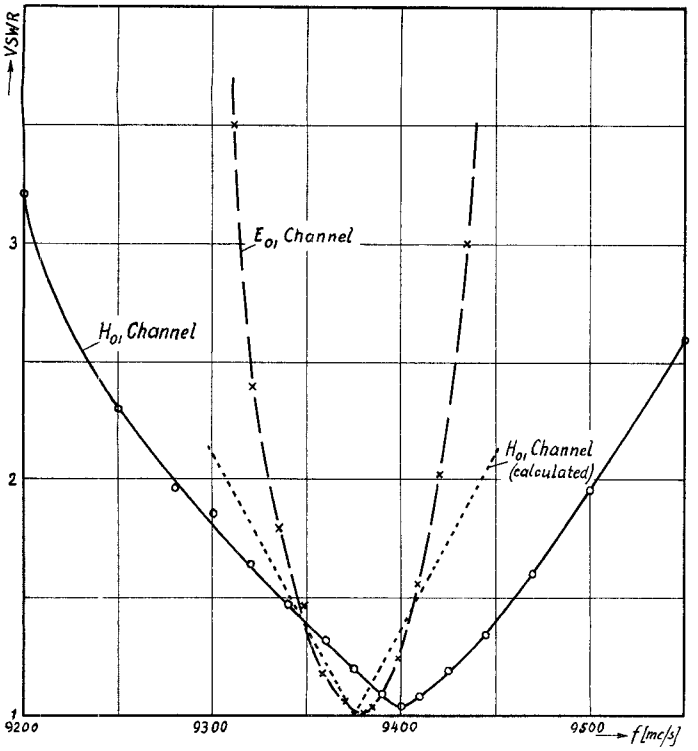


Fig. 10—VSWR-vs-frequency curves for the double rotary joint.

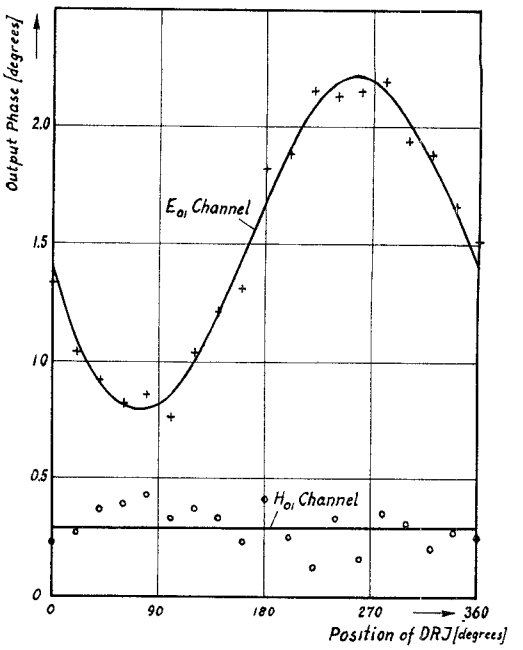


Fig. 11—Phase variation of the output of the two channels of the double rotary joint.

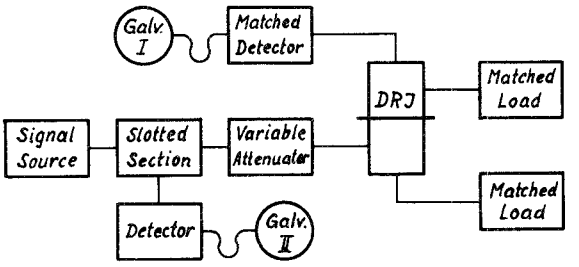


Fig. 12—Circuit for measuring the crosstalk between the two channels of a double rotary joint.

of the feeder waveguide, namely 0.900 inch $\times$0.400 inch. A tapered waveguide section served as a matching device between the feeder and the ring.

The diameter of the circular waveguide was determined by the required length of the waveguide ring which equals four guide wavelengths, resulting in a diameter of 1.75 inches. Coupling slots inside the circular waveguide were set at a distance of one guide wavelength—2.63 inches. With the additional two termination sections of one quarter-wavelength, total circular waveguide length became 3.94 inches, but preliminary tests showed that perfect match at the frequency of 3.975 mc required a slightly longer cavity of 4.06 inches.

*Measurement of VSWR vs Frequency*

The VSWR vs frequency is plotted in Fig. 10 for both channels. The bandwidth at a vswr of 2 is 90 mc for the $E_{01}$ channel and 225 mc for the $H_{01}$ channel. The shape of the curve for the $H_{01}$ channel around the minimum is nearly triangular as expected for a system in which resonance takes place. The theoretical curve is represented by the dotted line and shows fair agreement with the measurements. The higher slope of the theoretical curve is partly due to too large a value for the impedance ratio a result of assuming that the slots are extended over the full width of the rectangular waveguide. Hardly any variation of the VSWR curve with respect to the angular position of the DRJ could be measured.

*Measurement of the Phase of the Transmitted Signal*

The phase angle between the input and output of the two channels of the DRJ is shown in Fig. 11. The phase variations of the $H_{01}$ channel are not greater than the sensitivity of the measuring method which is 0.1 degree. However, the $E_{01}$ channel shows a slight sinusoidal variation. This is obviously due to mechanical imperfections because the maximum variation of $\pm$0.7 degree occurs in positions of perfect symmetry of the design.

*Measurement of the Crosstalk between Both Channels*

The crosstalk between the two channels is defined as the power ratio of the output leakage power in the secondary channel to the power in the primary channel. The circuit is illustrated in Fig. 12. A cw-signal supplied by the signal source is fed through a slotted section and a variable attenuator, into the DRJ ($H_{01}$). The output of this channel is terminated by a matched load. The probe of the slotted section is connected to a detector and a galvanometer. The input of the secondary channel of the DRJ is also terminated by a matched load, while the output is connected to a matched detector and galvanometer. Before measurements were taken

the outputs of the DRJ were interchanged. The attenuator was adjusted so that maximum deflection of the galvanometer (I) was obtained. The probe of the slotted section was also adjusted so that galvanometer (II) read maximum deflection. When taking measurements the attenuation was to be reduced until galvanometer (I), now in the secondary channel, showed maximum deflection. However, for most conditions, crosstalk was higher than the previous setting of the attenuator, so that additional attenuation was obtained from the actual deflection of the galvanometer (I) after the attenuator was set to zero. It was found that the detector characteristic followed the square law with sufficient accuracy that attenuation could be calculated.

Fig. 13 is a graphical presentation of the crosstalk vs angular position of the DRJ for three frequencies. Except for a series of narrow maxima, the crosstalk stays below the $-50$ db level. However, the maxima in the center of the band go up as high as $-47$ db, and never exceed $-42$ db at any frequency. The distribution of these maxima is regular insofar as they show up in pairs. The pairs are repeated every 90 degrees so that they are centered in the positions 45, 135, 225, and 315 degrees. It is supposed that these spike-shaped maxima result from resonance effects between network components of the two transmission circuits with interaction of undesired modes.

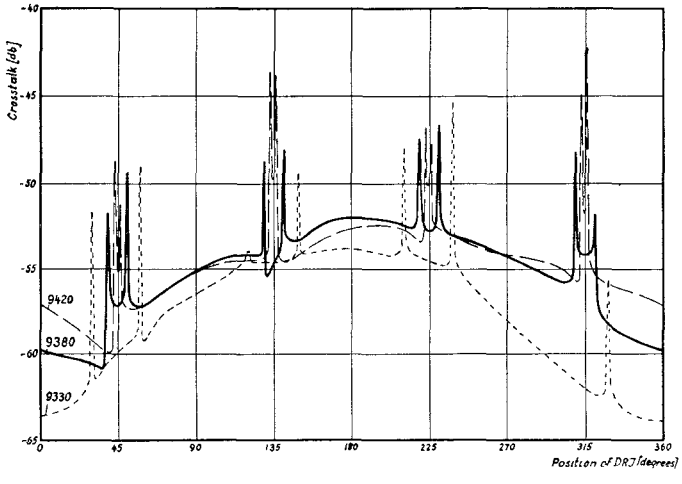


Fig. 13—Crosstalk between the two channels vs angular position for three different frequencies.

*Directions of Future Improvements*

Although this second model is far from an optimum design, it may serve as a useful new device in most cases. Better performance could be obtained with respect to the bandwidth and the crosstalk. The limitations due to unbalanced excitation of the slots as outlined above may become significant if the bandwidth is to be increased considerably. In this case the feeding of the slots must be modified as proposed. However, even with the simple feeding ring, improvements can be obtained by two methods: (1) Further reduction of the equivalent characteristic impedance ratio; (2) Use of additional circuit elements to match the rectangular and circular waveguides.

Method (1) means, for example, a further reduction of the radius of the circular waveguide. At the same time the height of the rectangular waveguide is to be increased. In other words, the VSWR as in (74) must be minimized, which means $\alpha$ in (69) must be set zero. The analytical solution of this problem becomes rather involved and it is questionable whether the result is useful, because some of the assumptions which simplified the analysis depend on narrow bandwidth or greater impedance ratio.

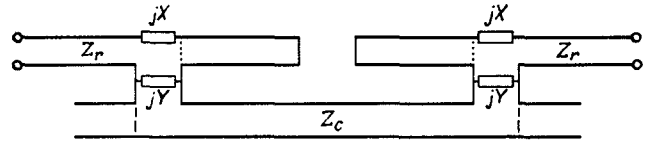


Fig. 14—Equivalent circuit for the $H_{01}$ channel of the double rotary joint with additional circuit elements for a broader band.

Method (2) could consist in a modification of a narrow-band rotary joint by adding some reactive components to the original equivalent circuit as Fig. 14 shows. Numerical values indicate that the effect of the resonance window can be neglected. Also, the quarter-wavelength cylindrical waveguide sections are of minor importance, so that they can be replaced by a short circuit along the dashed lines. The series reactances $jX$ can be realized simply by inserting a short circuit somewhere within the one wavelength rectangular waveguide sections. This means that these waveguide sections can be eliminated from the equivalent circuit as the dotted lines indicate. The parallel reactances $jY$ can be realized by nonresonant coupling windows.

The analysis of this circuit leads to the following conditions for perfect match

$$Y = -X - \frac{Z_r^2}{X} \quad \text{and} \quad X = \sqrt{Z_r(Z_c - Z_r)}.$$

These equations show that either kind of reactance, capacitive as well as inductive, can be used. However, if one kind is chosen as series reactance, the parallel reactance must be of the other kind.

## Appendix I

### Calculation of the Ratio of the Characteristic Impedance of the Transmission Lines Involved in the Equivalent Circuit for the $H_{01}$ Channel of the Double Rotary Joint

The electromagnetic wave of the $H_{10}$ mode in a rectangular waveguide as shown in Fig. 15(a), facing, is described by the three space components of the electric and magnetic field as follows:

$$\left.\begin{aligned} E_x &= E_z = H_y = 0, \\ E_y &= -B_r \frac{\mu_0 \omega a}{\pi} \sin \frac{\pi x}{a} \cdot \sin(\omega t - \beta_r z), \\ H_x &= B_r \frac{\beta_r a}{\pi} \cdot \sin \frac{\pi x}{a} \cdot \sin(\omega t - \beta_r z), \\ H_z &= -B_r \cos \frac{\pi x}{a} \cdot \cos(\omega t - \beta_r z), \end{aligned}\right\} \quad (1)$$

where $\mu_0 = 1.2560\ 10^{-8}\ Hy\ cm^{-1}$; the phase constant is

$$\beta_r = \sqrt{\frac{\omega^2}{c^2} - \frac{\pi^2}{a^2}} = \frac{2\pi}{\lambda_r}, \quad (2)$$

with $\lambda_r$ being the wavelength in the guide. $B_r$ is an arbitrary constant of amplitude.

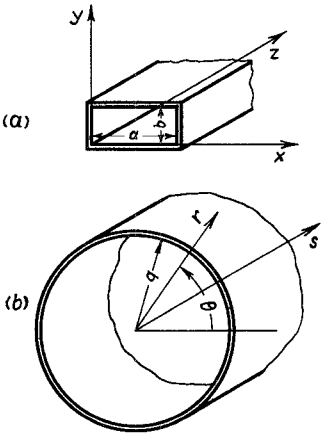


Fig. 15—The field co-ordinates of the rectangular (a) and the circular (b) waveguide as used in the double rotary joint.

The power of the transmission can be obtained from the Poynting vector

$$P_{zr} = E_y H_x = B_r^2 \frac{\mu_0 \omega \beta_r a^2}{2\pi^2} \sin^2 \frac{\pi x}{a} [1 - \cos 2(\omega t - \beta_r z)]. \quad (3)$$

The instantaneous power is

$$n_z = \int_{x=0}^{x=a} \int_{y=0}^{y=b} P_z dx dy = B_r^2 \frac{\mu_0 \omega \beta_r a^3 b}{4\pi^2} [1 - \cos 2(\omega t - \beta_r z)]. \quad (4)$$

Hence, the average power becomes

$$N_z = \frac{\omega}{\pi} \int_{t=0}^{t=(\pi/\omega)} n_z dt = B_r^2 \frac{\mu_0 \omega \beta_r a^3 b}{4\pi^2}. \quad (5)$$

The longitudinal wall-current density $s_r$ is equal to the transversal magnetic field component $H_x$ on the surface:

$$s_r = H_x. \quad (6)$$

If we express $H_x$ in terms of the power $N$, we have

$$s_r = 2 \sqrt{\frac{\beta_r N}{\mu_0 \omega a b}} \sin \frac{\pi x}{a} \cdot \sin(\omega t - \beta_r z). \quad (7)$$

Since we are especially interested in the current density along the center line of the slot, i.e. for $z = \text{const}$, we simplify the formula by setting $z = 0$ in the center of the slots. Hence the current density at the slot becomes

$$s_r = 2 \sqrt{\frac{\beta_r N}{\mu_0 \omega a b}} \cdot \sin \frac{\pi x}{a} \cdot \sin \omega t. \quad (8)$$

For the electromagnetic wave of the $H_{01}$ mode in the circular waveguide as illustrated in Fig. 15(b) the three space components of the electric and magnetic field are described as follows:

$$\left.\begin{aligned} E_r &= E_s = H_\theta = 0, \\ E_\theta &= B_c \mu_0 \frac{\omega q}{\rho} J_1\left(\rho \frac{r}{q}\right) \cdot \sin(\omega t - \beta_c s + \phi), \\ H_r &= B_c \frac{\beta_c q}{\rho} J_1\left(\rho \frac{r}{q}\right) \cdot \sin(\omega t - \beta_c s + \phi), \\ H_s &= -B_c J_0\left(\rho \frac{r}{q}\right) \cdot \cos(\omega t - \beta_c s + \phi), \end{aligned}\right\} \quad (9)$$

where the phase constant $\beta_c$ is

$$\beta_c = \sqrt{\frac{\omega^2}{c^2} - \frac{\rho^2}{q^2}} = \frac{2\pi}{\lambda_c}, \quad (10)$$

with $\lambda_c$ being the wavelength in the guide. $\rho = 3.832$ is the first zero for the first-order Bessel function, i.e. $J_1(\rho) = 0$. $B_c$ is an arbitrary constant of amplitude. The phase $\phi$ will be determined later so that the wall-current density in the center of the slot is of the same phase as the wall-current density due to the rectangular mode.

Again the power of the transmission can be obtained from the Poynting vector

$$P_s = E_\theta H_r = B_c^2 \frac{\mu_0 \omega \beta_c q^2}{\rho^2} \cdot J_1^2\left(\rho \frac{r}{q}\right) \frac{1}{2} [1 - \cos 2(\omega t - \beta_c s + \phi)]. \quad (11)$$

The instantaneous power is

$$n_s = \int_{\theta=0}^{\theta=2\pi} \int_{r=0}^{r=q} P_s r d\theta dr = B_c^2 \frac{\mu_0 \omega \beta_c q}{\rho^2} \pi q^2 J_0^2(\rho) \frac{1}{2} [1 - \cos 2(\omega t - \beta_c s + \phi)]. \quad (12)$$

Because of $J_0(\rho) = 0.4028$ we can write

$$n_s = \mu_0 \omega \beta_c \pi \left(\frac{B_c q^2 0.4028}{\rho}\right)^2 \frac{1}{2} [1 - \cos 2(\omega t - \beta_c s + \phi)]. \quad (13)$$

Hence the average power becomes

$$N_s = \frac{\mu_0 \omega \beta_c \pi}{2} \left(\frac{0.4028 B_c q^2}{\rho}\right)^2. \quad (14)$$

The transverse wall-current density $s_c$ is equal to the longitudinal magnetic field $H_s$ on the surface:

$$s_c = H_s. \tag{15}$$

If we express $H_s$ in terms of the power $N_s$, we have

$$s_c = -\frac{\rho}{q^2}\sqrt{\frac{2N_s}{\mu_0\omega\beta_c\pi}}\cos(\omega t - \beta_c s + \phi). \tag{16}$$

If we assume that the rotary joint is designed so that the longitudinal wavelength in the circular guide is equal to the transverse wavelength, which means

$$\beta_c = \frac{\pi}{a}, \tag{17}$$

and, if we neglect the fact that the phase of the current density in the circular guide varies along the slot as indicated by this variable $s$, we may compare the wall-current density waves by forming the ratio of the amplitudes $s_{r\max}$ and $s_{c\max}$. If $N_r = N_s = N$, this ratio becomes

$$\frac{s_{r\max}}{s_{c\max}} = \frac{q^2}{\rho}\sqrt{\frac{2\pi\beta_r\beta_c}{ab}}. \tag{18}$$

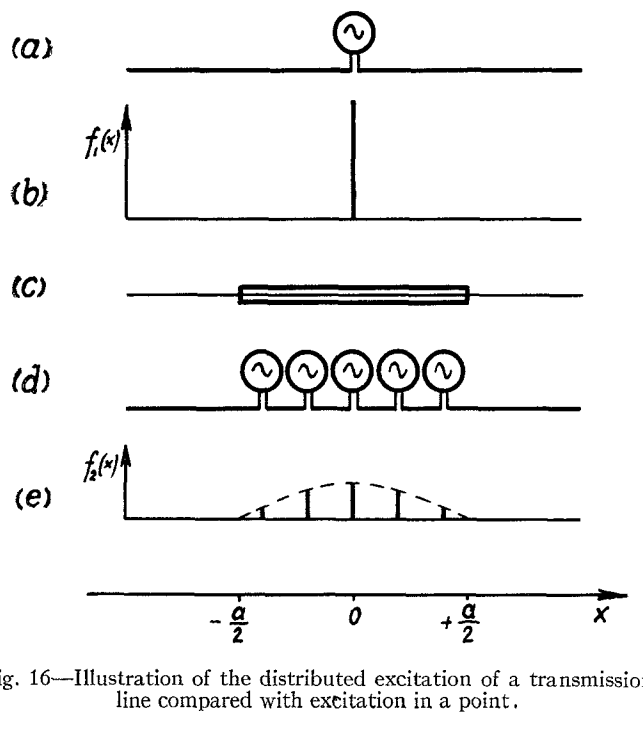


Fig. 16—Illustration of the distributed excitation of a transmission line compared with excitation in a point.

The actual situation is illustrated in Fig. 16. If the current enters the cylinder wall over an extremely short length, the equivalent network would be a single source as in (a) with a differential voltage function (b). But since the coupling occurs over the full length of the slot, which for simplicity is thought to be extended over the full width of the rectangular waveguide as in (c) we have an infinite number of generators along the length of the slot as in (d), which produce a sinusoidal voltage distribution as shown in (e).

In order to calculate the ratio between the current in the line produced by a distributed system of generators and the current produced by the single generator, we first state that the stationary voltage integral is the same in both cases. We now have the two differential voltage functions:

$$\left.\begin{aligned} f_1(x)dx &= U\sin\omega t, \quad x = 0 \\ f_1(x)dx &= 0, \qquad\quad x \neq 0 \end{aligned}\right\} \tag{19}$$

and

$$\left.\begin{aligned} f_2(x)dx &= u\cos\frac{\pi}{a}x\cdot\sin\omega t dx, \quad |x| \leq \frac{a}{2} \\ f_2(x)dx &= 0, \qquad\qquad\qquad |x| > \frac{a}{2} \end{aligned}\right\}. \tag{20}$$

Hence

$$\int_{-a/2}^{+a/2} f_1(x)dx = \int_{-a/2}^{+a/2} f_2(x)dx. \tag{21}$$

This means

$$U\sin\omega t = \int_{-a/2}^{+a/2} u\cos\frac{\pi}{a}x\cdot\sin\omega t dx \tag{22}$$

or

$$U = 2\frac{a}{\pi}u. \tag{23}$$

Therefore,

$$f_2(x) = \frac{\pi}{2a}U\cos\frac{\pi}{a}x\cdot\sin\omega t. \tag{24}$$

In a point located on the line at the arbitrary distance $x = s$, $s > (a/2)$ we have the line current due to $f_1(x)$:

$$i_{1s} = \frac{U}{2Z_c}\sin(\omega t - \beta_c s). \tag{25}$$

The line current at the same point due to $f_2(x)$ becomes

$$i_{2s} = \frac{\pi U}{4aZ_c}\int_{-a/2}^{+a/2}\cos\frac{\pi}{a}x\cdot\sin[\omega t - \beta_c(s-x)]dx. \tag{26}$$

In order to carry out the integration the trigonometrical function must be transformed so that

$$i_{2s} = \frac{\pi U}{4aZ_c}\left[\sin(\omega t - \beta_c s)\int_{-a/2}^{+a/2}\cos\frac{\pi}{a}x\cdot\cos\beta_c x dx + \cos(\omega t - \beta_c s)\int_{-a/2}^{+a/2}\cos\frac{\pi}{a}x\cdot\sin\beta_c x dx\right]. \tag{27}$$

The second term within the brackets is an odd function, so that this integral becomes zero. The first term can again be transformed so that

$$i_{2s} = \frac{\pi U}{8aZ_c}\sin(\omega t - \beta_c s)\left[\int_{-a/2}^{+a/2}\cos\left(\frac{\pi}{a} + \beta_c\right)x dx + \int_{-a/2}^{+a/2}\cos\left(\frac{\pi}{a} - \beta_c\right)x dx\right]. \tag{28}$$

The integration of this equation leads to

$$i_{2s}=\frac{\pi U}{8Z_c}\sin(\omega t-\beta_c s)\left\{\frac{\sin\frac{\pi+a\beta_c}{2}}{\frac{\pi+a\beta_c}{2}}+\frac{\sin\frac{\pi-a\beta_c}{2}}{\frac{\pi-a\beta_c}{2}}\right\}, \tag{29}$$

or

$$i_{2s}=\frac{\pi^2 U}{2Z_c(\pi^2-a^2\beta_c{}^2)}\cos\frac{a\beta_c}{2}\cdot\sin(\omega t-\beta_c s). \tag{30}$$

From (25) and (30) we obtain the ratio

$$r=\frac{i_{1s}}{i_{2s}}=\frac{\pi^2-a^2\beta_c{}^2}{\pi^2\cos\frac{\alpha\beta_c}{2}}\cdot \tag{31}$$

If the ratio of the characteristic impedances of the rectangular and circular waveguides is $1/p$, the current ratio is $\sqrt{p}$, if both waveguides conduct the same power. From this analysis, especially (18) and (31), we obtain

$$\sqrt{p}=\frac{s_{r\max}}{s_{c\max}}\cdot r=\frac{q^2(\pi^2-a^2\beta_c{}^2)}{\pi\rho\cos\frac{a\beta_c}{2}}\sqrt{\frac{2\beta_r\beta_c}{\pi ab}}, \tag{32}$$

or

$$p=\frac{4q^4\beta_r\beta_c(\pi^2-a^2\beta_c{}^2)^2}{\pi^3\rho^2 ab(1+\cos a\beta_c)}\cdot \tag{33}$$

## Appendix II

### Calculation of the Slope of the VSWR vs Frequency Curve for the $H_{01}$ Channel of the Double Rotary Joint

We assume that the DRJ is terminated by a matched load as Fig. 8 shows. We would like to know the VSWR at the input to the $H_{01}$ channel of the DRJ. This means that we first must calculate the input impedance $Z_i$ of the rotary joint. In order to do this we start at the load and calculate the internal impedances of the equivalent network in progressing steps. If this is done rigorously the equations for these impedances become more and more complicated even if we consider the internal losses as negligible. Since the experimental VSWR curve is almost linear around the operating frequency, the analysis can be much simplified if we restrict it to the calculation of the slope of the VSWR curve at the operating frequency. Therefore, we introduce the normalized frequency deviation $k$ from the operating frequency 1, as defined by

$$k=\frac{\omega-\omega_0}{\omega_0}=\frac{f-f_0}{f_0}\cdot \tag{34}$$

If all internal impedances are expressed as a function of $k$ we have to consider only the constant and linear terms.

At the first slot the shunt impedance of the equivalent network consists of the load impedance $z_1=z_r$ plus the impedance of the short-circuited waveguide stub, one wavelength $\lambda_{0c}$ long:

$$Z_2=Z_r\tanh\gamma_r\lambda_{0c}, \tag{35}$$

where the propagating constant is

$$\gamma_r=j\beta_r=j\frac{2\pi}{\lambda_r}=j\frac{2\pi}{\lambda}\sqrt{1-\frac{\lambda^2}{4a^2}}\cdot \tag{36}$$

We can express $\lambda$ in terms of $k$ as defined in (34) and set

$$\lambda=\frac{\lambda_0}{1+k}\cdot \tag{37}$$

If this term is substituted for $\lambda$ in (36) we will have

$$\gamma_r=j\frac{2\pi}{\lambda_0}\sqrt{(1+k)^2-\frac{\lambda_0{}^2}{4a^2}}\cdot \tag{38}$$

Since $k$ is small we may write the approximation

$$\gamma_r\simeq j\frac{2\pi}{\lambda_0}\sqrt{1-\frac{\lambda_0{}^2}{4a^2}}\left(1+\frac{k}{1-\frac{\lambda_0{}^2}{4a^2}}\right)$$

$$=j\frac{2\pi}{\lambda r_0}(1+rk). \tag{39}$$

This equation shows that the propagation constant varies with frequency in a different way from that of an ideal transmission line, in which case the factor

$$r=\frac{1}{1-\frac{\lambda_0{}^2}{4a^2}} \tag{40}$$

is 1. For a waveguide, $r>1$ means that the phase change with frequency is greater than that of an ideal transmission line, and consequently the bandwidth will be narrower than if we consider the equivalent circuit to consist of ideal transmission line sections.

If we substitute $\gamma_r$ as in (35) by (38) we obtain

$$Z_2=jZ\tan 2\pi(1+rk)=jZ_r\tan 2rk\pi, \tag{41}$$

or

$$Z_2\simeq j2rk\pi Z_r. \tag{42}$$

Therefore, the shunt impedance to the slot becomes

$$Z_3=Z_r(1+j2rk\pi). \tag{43}$$

Hence, the admittance $S_3=1/Z_3$ will become

$$S_3=\frac{1}{Z_r(1+j2rk\pi)}\simeq\frac{1}{Z_r}(1-j2rk\pi). \tag{44}$$

The slot itself represents a shunt susceptance $S_s$ of a capacitor and an inductor. Both are in resonance with the operating frequency so that the susceptance is

$$S_s=j\left(\omega C_s-\frac{1}{\omega L_s}\right). \tag{45}$$

With $\omega=\omega_0(1+k)$ and the resonance condition $\omega_0 L_s = 1/\omega_0 C_s$ we derive

$$S_s = j2k\omega_0 C_s. \tag{46}$$

The dimensions of the slots, 0.66 inch $\times$ 0.128 inch, have been obtained from an empirical formula. Since no analysis of the slot impedance was available, it was estimated from calculations for capacitive and inductive windows of comparable size. Thus

$$\omega_0 C_s = 0.5/Z_r. \tag{47}$$

Hence

$$S_s = j\frac{k}{Z_r}. \tag{48}$$

Now we obtain the admittance in position (4) of the equivalent circuit as

$$S_4 = S_3 + S_s = \frac{1}{Z_r}[1 - jk(2\pi r - 1)]. \tag{49}$$

The respective impedance becomes

$$Z_4 = Z_r[1 + jk(2\pi r - 1)]. \tag{50}$$

The reactance of the open-end circular waveguide, which is a quarter-wavelength long, is

$$Z_5 = Z_c \coth \gamma_c \frac{\lambda_{0c}}{4}, \tag{51}$$

where the propagation constant is

$$\gamma_c \simeq j\beta_c = j\frac{2\pi}{\lambda_c} = j\frac{2\pi}{\lambda}\sqrt{1 - \frac{\lambda^2\rho^2}{4\pi^2 q^2}}. \tag{52}$$

As above, we replace $\lambda$ by (37) and derive approximation

$$\gamma_c \simeq j\frac{2\pi}{\lambda_0}\sqrt{1 + \frac{\lambda_0^2\rho^2}{4a^2q^2}}\left(1 + \frac{k}{1 - \frac{\lambda_0^2\rho^2}{4a^2q^2}}\right)$$

$$= j\frac{2\pi}{\lambda_{c0}}(1 + ck), \tag{53}$$

where

$$c = \frac{1}{1 - \frac{\lambda_0^2\rho^2}{4a^2q^2}} \tag{54}$$

is to the circular waveguide what $r$ is to the rectangular guide. With $\gamma_c$ as of (53) inserted in (51) we obtain:

$$Z_5 = -jZ_c \cot\frac{\pi}{2}(1 + ck) = jZ_c \tan\frac{ck\pi}{2}, \tag{55}$$

and

$$Z_5 \simeq j\frac{ck\pi}{2}Z_c. \tag{56}$$

In Appendix I the ratio $Z_c/Z_r$ was calculated and denoted by $p$, so that

$$Z_5 = j\frac{ck\pi}{2}pZ_r. \tag{57}$$

In position (6) of the equivalent circuit we have the impedances $Z_4$ and $Z_5$ in series so that

$$Z_6 = Z_4 + Z_5 = \left[1 + jk\left(2\pi r - 1 + \frac{c\pi p}{2}\right)\right]Z_r. \tag{58}$$

This impedance represents the load of the circular waveguide for which we can calculate the input impedance $Z_7$ by means of the formula

$$Z_7 = \frac{Z_6 \cosh \gamma_c\lambda_{0c} + Z_c \sinh \gamma_c\lambda_{0c}}{\cosh \gamma_c\lambda_{0c} + \frac{Z_c}{Z_c}\sinh \gamma_c\lambda_{0c}}. \tag{59}$$

As in previous operations we simplify this equation and obtain

$$Z_7 = \frac{Z_6 \cos 2ck\pi + jpZ_r \sin 2ck\pi}{\cos 2ck\pi + j\frac{Z_6}{pZ_r}\sin 2ck\pi}. \tag{60}$$

Hence

$$Z_7 \simeq \frac{Z_6 + j2ck\pi pZ_r}{1 + j2ck\pi\frac{Z_6}{pZ_r}} \simeq Z_6 + j2ck\pi\left(pZ_r - \frac{Z_6^2}{pZ_r}\right). \tag{61}$$

Here we replace $Z_6$ by (58) and obtain

$$Z_7 = \left[1 + jk\left(2\pi r - 1 + \frac{5c\pi p}{2} - \frac{2c\pi}{p}\right)\right]Z_r. \tag{62}$$

The shunt impedance to the transmitting slots $Z_8$ is

$$Z_8 = Z_7 + Z_5 = \left[1 + jk\left(2\pi r - 1 + 3c\pi p - \frac{2c\pi}{p}\right)\right]Z_r. \tag{63}$$

In order to obtain the impedance across the slots we first form the admittance

$$S_8 = \frac{1}{Z_8} = \left[1 - jk\left(2\pi r - 1 + 3c\pi p - \frac{2c\pi}{p}\right)\right]\frac{1}{Z_r}, \tag{64}$$

and add the slot susceptance $S_s$ to obtain

$$S_9 = S_8 + S_s = \left[1 - jk\left(2\pi r - 2 + 3c\pi p - \frac{2c\pi}{p}\right)\right]\frac{1}{Z_r}. \tag{65}$$

Hence

$$Z_9 = \frac{1}{S_9} = \left[1 + jk\left(2\pi r - 2 + 3c\pi p - \frac{2c\pi}{p}\right)\right]Z_r. \tag{66}$$

Finally the input impedance can be obtained by adding $Z_2$ to the slot impedance:

$$Z_i = Z_9 + Z_2 = \left[1 + jk\left(4\pi r - 2 + 3c\pi p - \frac{2c\pi}{p}\right)\right]Z_r. \tag{67}$$

In a short form we can write

$$Z_i = (1 + j\alpha k)Z_r, \tag{68}$$

where

$$\alpha = 4\pi r - 2 + 3c\pi p - \frac{2c\pi}{p}. \tag{69}$$

According to these equations perfect match $Z_i = Z_r$ can be obtained at the operating frequency ($k = 0$), as it was anticipated. The reactive component is determined by $\alpha$ which is a function of the impedance ratio $p$.

In order to set up the relation between the VSWR, $R$ and $\alpha$, we first calculate the reflection coefficient

$$\Gamma = \frac{Z_i - Z_r}{Z_i + Z_r}. \tag{70}$$

If we use the relation of (68) we obtain

$$\Gamma = \frac{j\alpha k}{2 + j\alpha k}. \tag{71}$$

The VSWR can now be expressed in terms of $\Gamma$[1]

$$R = \frac{1 + |\Gamma|}{1 - |\Gamma|}. \tag{72}$$

Substituting (71) in (72) gives

$$R = \frac{\sqrt{4 + \alpha^2 k^2} + \alpha k}{\sqrt{4 + \alpha^2 k^2} - \alpha k}. \tag{73}$$

Neglecting higher orders of $k$ than the first we obtain the simple function

$$R = 1 + \alpha k. \tag{74}$$

Therefore, $\alpha$ directly determines the slope of the vswr curve around the operating frequency.

[1] C. G. Montgomery, "Technique of Microwave Measurements," Radiation Laboratory Series, vol. 11, McGraw-Hill Book Co., Inc., New York, N. Y.; 1947.

# Transverse Electric Resonances in a Coaxial Line Containing Two Cylinders of Different Dielectric Constant

J. W. CARR†

*Summary*—**A coaxial line containing a medium of propagation consisting of two coaxial cylindrical cylinders of different dielectric constant is considered for the special case of $TE_{nm}$ resonances, and numerical calculations are carried out for a few cases of the $TE_{11}$ type resonance. A reference paper called to the attention of the author by the reviewer treats the general condition of propagation in such a line. The numerical solutions to the cases of interest in this application were not performed, however, presumably since the interest was in propagating modes and since the general characteristic equation is quite complicated. It is shown here that consideration of transverse boundary conditions only leads to an equation which is much less complicated and which is equivalent to the reduction of the general characteristic equation (of the reference paper) when cutoff is approached.**

## Introduction

USING coaxial chokes in the upper microwave region, difficulty is encountered due to the presence of higher-order mode resonances in the choke sections. At these shorter wavelengths it is quite difficult to maintain a rugged mechanical construction of the transmission system, including the choke, and prevent occurrence of the circumferential $TE_{11}$ resonance in the choke sections while operating the system over a broad band. In design literature ways of damping out this undesirable resonance are indicated. However, this usually leads to a tedious experimental project and results in a choke design which is quite complicated and not very rugged mechanically. For the ratios of outer to inner diameters used in such chokes containing a single homogeneous isotropic medium the $TE_{11}$ and $TE_{21}$ resonances are the first two that are excited in the choke as the operating frequency is increased. They are separated spectrally by a nearly two-to-one ratio for the diameter ratios (under 2 to 1) used in chokes.

If we are justified in assuming that a medium consisting of two concentric cylinders of different dielectric constant maintains essentially the same relative spectral separation between the $TE_{11}$ and $TE_{21}$ resonances, then only the calculations for the $TE_{11}$ resonant conditions need be made.

Rather than make the whole structure very small, or use the resonance damping technique, the effective medium of the choke can be changed by partial dielectric loading (partial to allow clearance for mechanical rotation and eccentricities) so that the $TE_{11}$ resonance comes in below the band of operation and the $TE_{21}$ above the band. The resulting design can be kept quite

† Gilfillan Brothers, Inc., Los Angeles, Calif.